

Eqs. (8) and (9) yields, after some manipulation,

$$P^{(e)} = \sum_n \left\{ \frac{(a_n - b_n)^2}{2} + 2a_n b_n \sin^2 \left[\frac{(\beta_n - \alpha_n)}{2} \right. \right. \\ \left. \left. + \frac{1}{\hbar} \int_{R_c}^{\infty} \frac{\Delta_n(R)}{v(R)} \left(1 - \frac{v(\infty)^2 S^2}{v(R)^2 R^2} \right) dR \right] \right\}, \quad (12)$$

where

$$\Delta_n(R) = \epsilon_n^+(R) - \epsilon_n^-(R). \quad (13)$$

For charge exchange without excitation the probability is obtained by substituting Eqs. (10) into (12) and yields Eq. (1).

Examination of Eq. (12) shows that if the following two conditions hold for most of the excited states which have appreciable amplitude:

$$\begin{aligned} \Delta_n(R) &\simeq \Delta_0(R), \\ c_n^+(S) &\simeq c_n^-(S), \end{aligned} \quad (14)$$

then

$$a_n b_n = |c_n^+|^2 = |c_n^-|^2, \quad (15)$$

and it follows that

$$\begin{aligned} P^{(e)} &= \left(\sum_n (|c_n^+|^2 + |c_n^-|^2) \right) \sin^2 \left[\frac{1}{\hbar} \int_{R_c}^{\infty} \frac{\Delta_0(R)}{v(R)} \right. \\ &\quad \left. \times \left(1 - \frac{v(\infty)^2 S^2}{v(R)^2 R^2} \right) dR \right] \\ &= \sin^2 \left[\frac{1}{\hbar} \int_{R_c}^{\infty} \frac{\Delta_0(R)}{v(R)} \left(1 - \frac{v(\infty)^2 S^2}{v(R)^2 R^2} \right) dR \right]. \end{aligned} \quad (16)$$

Thus, if Eqs. (14) are true, then the probability of electron exchange with excitation will turn out to be exactly the same as that predicted for electron exchange without excitation.

4. ACKNOWLEDGMENTS

We wish to express our appreciation to Dr. Edgar Everhart for several helpful discussions.

(p, n) Cross Section and Proton Optical-Model Parameters in the 4- to 5.5-Mev Energy Region*

RICHARD D. ALBERT

University of California, Lawrence Radiation Laboratory, Livermore, California

(Received March 23, 1959)

(p, n) cross sections were measured for 18 medium-weight nuclei in the 4- to 5.5-Mev region. In this energy region, de-excitation of the compound nucleus by neutron emission is largely favored over charged particle emission; consequently, the (p, n) reaction dominates competing compound-elastic and inelastic scattering processes. The experimental results are compared with theoretical reaction cross sections predicted by the optical model for protons. It is found that the parameters which provide the best theoretical fit to these data also provide reasonable fits to neutron total, nonelastic, and elastic cross sections measured elsewhere when the latter are compared with theoretical cross sections predicted by the optical model for neutrons. It is concluded that the intrinsic nuclear well depth for protons and neutrons are equal to within $\pm 7\%$ uncertainty.

IN the optical model,¹⁻⁵ the interaction between an incident nucleon and a target nucleus is approximated by means of a potential well. The ensuing behavior may be described in terms of a differential scattering cross section and a reaction cross section which are derived from solution of the Schrödinger equation containing a complex potential. The reaction cross section is composed of contributions from both nonelastic and compound-elastic nuclear processes. Both of these components describe nuclear processes in which the incident neutron leaves its entrance channel; compound

elastic scattering occurs when the entrance and final channels are the same.

It has been pointed out by several investigators^{6,7} that the proton differential elastic scattering experiments performed in the low-energy region are difficult to interpret satisfactorily by standard methods using optical-model theory. It is felt that the observed anomalous behavior in the proton angular distribution is caused, at least partially, by effects due to compound elastic scattering.⁷ Interpretation of proton reaction

* Work performed under the auspices of U. S. Atomic Energy Commission.

¹ H. A. Bethe, Phys. Rev. **57**, 1125 (1940).

² Fernbach, Serber, and Taylor, Phys. Rev. **75**, 1352 (1949).

³ H. H. Barschall, Phys. Rev. **86**, 431 (1952).

⁴ Feshbach, Porter, and Weisskopf, Phys. Rev. **96**, 448 (1954).

⁵ R. D. Woods and D. S. Saxon, Phys. Rev. **95**, 577 (1954).

⁶ D. A. Bromley and N. S. Wall, Phys. Rev. **99**, 1029 (1955), and **102**, 560 (1956); Greenlees, Haywood, Kuo, and Petravic, Proc. Phys. Soc. (London) **A70**, 331 (1957).

⁷ W. F. Waldorf and N. S. Wall, Phys. Rev. **107**, 1602 (1957); C. A. Preskitt and W. P. Alford, University of Rochester, New York, Atomic Energy Commission Report NYO-2172, March 17, 1958 (unpublished).

cross sections in this energy region by means of optical-model theory has not been attempted previously.

For this experiment the incident proton energy is well above the threshold for neutron emission and below the height of the Coulomb barrier. In this energy region, de-excitation of the compound nucleus by neutron emission is largely favored over charged particle emission; consequently, the (p,n) reaction dominates competing compound-elastic and inelastic scattering processes. Therefore, it seems reasonable to compare results of (p,n) cross section measurements with optical-model predictions of proton reaction cross sections.

Thin targets (about 1 mg/cm²) of the elements to be investigated were evaporated on tantalum backings thick enough to stop the proton beam of the variable-energy Livermore 90-inch cyclotron. The results represent averages over many levels of the compound nucleus because of a proton energy spread of about 100 keV due to roughly equal contributions from degradation in the targets and natural inhomogeneity of the proton beam.

(p,n) cross sections in the region of atomic numbers 20 to 50 have been measured previously by a stacked-foil activation technique.⁸ Nuclei in this part of the periodic table are approximately spherical in shape. In the present arrangement, neutrons are detected by means of a "long counter"⁹ of approximately flat energy response located about 4 inches from target. Measurements of angular distributions indicate isotropic emission of neutrons from these targets within about 10%

instrumental error. In order to obtain cross sections, proton current was monitored to about 2% accuracy and the "long counter" was calibrated with a mock fission source having a strength known to about 5% accuracy. The final (p,n) cross section results are believed to be about 15% accurate.

Results for four proton energies are shown in Fig. 1. The experimental points are averages for several re-treated measurements. Important contributions to the cross sections of nickel and copper result from (p,n) thresholds occurring in the energy region being studied. Consequently, values for the isotopes Ni⁶⁴ and Cu⁶⁵ are plotted instead. Cross sections for these isotopes, which have (p,n) thresholds well below the energy region of interest, were obtained from the work of Blaser *et al.*,⁸ after it was found that their results and ours agree for these natural elements.

The optical-model potential is of the following type¹⁰:

$$U = V\rho(r) + iWq(r) + \frac{\lambda\hbar^2}{4m_0^2c^2} \frac{V}{r} \frac{d\rho}{dr} - \sigma \cdot \mathbf{l},$$

where

$$\rho(r) = [1 + \exp(r - R_0)/a]^{-1},$$

$$q(r) = \exp[-(r - R_0)^2/b^2],$$

$$R_0 = r_0A^{1/3}.$$

For protons there is an added term corresponding to the Coulomb potential arising from a uniform charge distribution in the nucleus of radius R_0 . The spin-orbit potential is the usual Thomas term multiplied by a constant, λ .

The theoretical fits to the experimental data of Fig. 1 were obtained using the optical-model parameters listed in Table I. The value of the spin-orbit interaction used in these calculations is about 35 times the Thomas term.

The experimental data are not corrected for contributions arising from charged-particle emission. Small deviations between the experimental data and the theoretical curve which occur in the light-element region may arise from neglect of these effects for nuclei having relatively large Coulomb penetrabilities. At 4 Mev, the calculations could not be extended beyond $Z=30$ since the approximate procedure for calculating

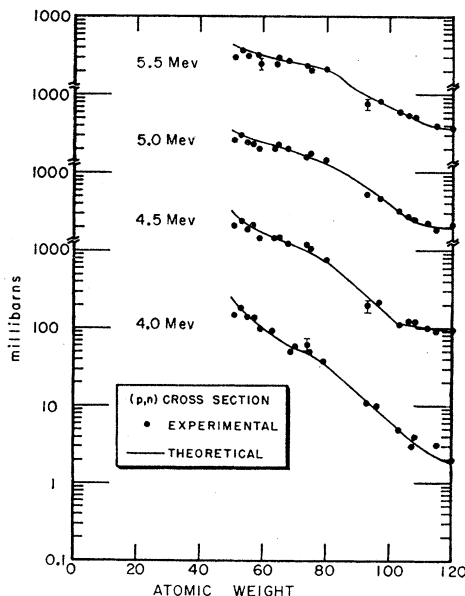


FIG. 1. (p,n) cross section vs atomic weight for protons of 5.5, 5.0, 4.5, and 4.0 Mev.

⁸ Blaser, Boehm, Marmier, and Scherrer, *Helv. Phys. Acta* **24**, 441 (1954); Blaser, Boehm, Marmier, and Peaslee, *Helv. Phys. Acta* **24**, 3 (1954); H. A. Howe, *Phys. Rev.* **109**, 2083 (1958).

⁹ A. O. Hanson and J. L. McKibben, *Phys. Rev.* **72**, 673 (1947).

TABLE I. Parameters adopted as giving the best fits to experimental data of Fig. 1. $a=0.65 \times 10^{-13}$ cm; $r_0=1.25 \times 10^{-13}$ cm; $b=0.98 \times 10^{-13}$ cm.

E (Mev)	V (Mev)	W (Mev)
5.5	44	8.7
5.0	45	8.25
4.5	45	7.7
4.0	47	7.0

¹⁰ F. Bjorklund and S. Fernbach, *Phys. Rev.* **109**, 1295 (1958). I should like to thank these authors for permission to use their IBM 704 optical-model code.

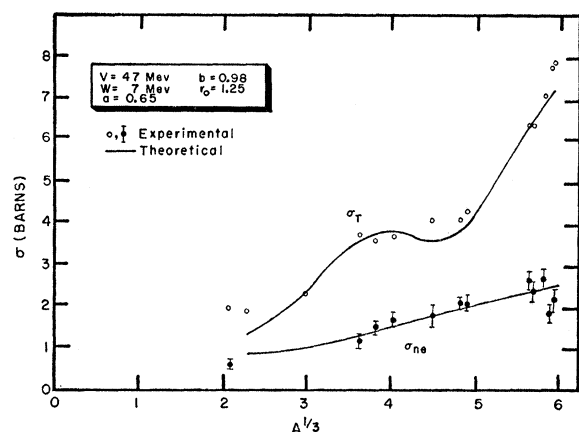


FIG. 2. Optical-model fit to experimental data of Beyster, Walt, and Salmi (reference 12) for neutron total and nonelastic cross sections at 4.1 Mev.

Coulomb wave functions used in the presently available code breaks down in this region.¹¹

Figures 2 and 3 are a comparison between theory and experiment for neutron total, nonelastic, and elastic cross sections measured by Beyster, Walt, and Salmi.¹² Attempts to fit previously measured angular distributions of proton elastic scattering⁷ were not successful. As previously noted,^{6,7} the experimental angular distributions change radically from element to element. It does not appear that these data can be fitted with a unique set of optical-model parameters unless corrections are made for some other effect, possibly compound elastic scattering.

It is worthy of note that optical-model theory provides reasonable fits to the previously obtained neutron experimental results as well as to the proton results of the present experiment if the same parameters are used for both protons and neutrons. Since, for small parameter variations, the optical-model fit is determined by the quantity Vr^2 rather than V and r separately, it may be concluded that if the neutron and proton potential wells have the same radius, they are equal in depth to an estimated $\pm 7\%$ uncertainty.

Information about the proton well has been previously obtained from analysis of proton "strength function" experiments.¹³ Schiffer and Lee found that the intrinsic proton well is 2.5 ± 2.5 Mev deeper than the neutron well. This result does not differ significantly from ours when the experimental errors are taken into

¹¹ I am very grateful to Dr. M. A. Melkanoff for providing the 4-Mev optical-model calculation (modified in proof) shown in Fig. 1.

¹² Beyster, Walt, and Salmi, Phys. Rev. **104**, 1319 (1956); M. Walt and J. R. Beyster, Phys. Rev. **98**, 677 (1955).

¹³ J. P. Schiffer and L. L. Lee, Jr., Phys. Rev. **107**, 640 (1957), and **109**, 2098 (1958); Johnson, Galonsky, and Ulrich, Phys. Rev. **109**, 1243 (1958); B. Margolis and V. F. Weisskopf, Phys. Rev. **107**, 641 (1957).

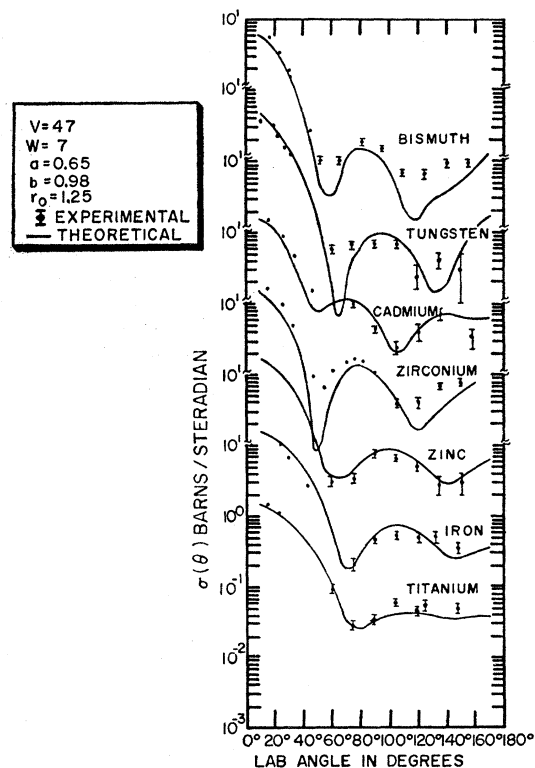


FIG. 3. Optical-model fit to experimental data of Walt and Beyster for neutron elastic scattering angular distributions at 4.1 Mev.

account. Johnson, Galonsky, and Ulrich found that the proton well is 4 Mev deeper than the neutron well. A deeper proton well can be supported by theoretical calculations.¹⁴ Since the over-all uncertainties are not quoted, it is difficult to say whether the difference between the latter result and ours is significant. However, within the experimental accuracy of the present experiment, we prefer to interpret the experimental evidence as indicating that the intrinsic proton and neutron wells are equal.

ACKNOWLEDGMENTS

Thanks are due many people who assisted in carrying out this experiment, in particular Darryl Malone, who helped run the experiment and analyze the data. I am also grateful to H. Brooks, R. Rhein, and L. Talbot for their aid in design of experimental equipment, D. Fraed and Barbara Hurlbut, who helped analyze data, and O. Tveitmo, H. Fong, D. Rawles, R. Benedict, D. Malone, R. Jones, A. Horn, and D. Telec of the cyclotron crew.

¹⁴ A. E. S. Green, Phys. Rev. **102**, 1325 (1956); **104**, 1617 (1956); Ross, Lawson, and Mark, Phys. Rev. **104**, 401 (1957).